Inorganic Chemistry

COMMUNICATION

pubs.acs.org/IC

A 3D Cu^{II} Coordination Framework with μ_4-/μ_2-Oxalato Anions and a Bent Dipyridyl Coligand: Unique Zeolite-Type NiP_2 Topological Network and Magnetic Properties

Miao Du,[*,†,‡] Zhi-Hui Zhang,[†] Cheng-Peng Li,[†] Jordi Ribas-Ariño,[§] Núria Aliaga-Alcalde,[⊥,#] and Joan Ribas[⊥]

[†]College of Chemistry, Tianjin Key Laboratory of Structure and Performance for Functional Molecule, Tianjin Normal University, Tianjin 300387, People's Republic of China

[‡]State Key Laboratory of Structural Chemistry, Fujian Institute of Research on the Structure of Matter, Chinese Academy of Sciences, Fuzhou, Fujian 350002, People's Republic of China

[§]Departament de Química Física and IQTCUB, Facultat de Química, [⊥]Departament de Química Inorgànica, and [#]ICREA Junior Researcher, Universitat de Barcelona, Diagonal 647, 08028 Barcelona, Spain

Supporting Information

ABSTRACT: The reaction of copper(II) nitrate, oxamide, and an angular bridging ligand 2,5-bis(4-pyridyl)-1,3,4-oxadiazole (4-bpo) under hydrothermal conditions affords a 3D pillared-layer coordination framework $\{[Cu_2(4\text{-bpo})(ox)_2](H_2O)_4\}_n$ (**1**) (ox = oxalate), featuring the unique zeolite-type NiP_2 network and interesting properties.

The design and construction of metal−organic frameworks (MOFs) is currently a flourishing research field because of their broad applications, especially as a new type of zeolite-analogous materials.[1] In zeolites, the cationic components Al^{3+} and Si^{4+} always feature tetrahedral geometry, indicating that a lower coordination number (<6) with more directional bonding prefers to construct an open crystalline lattice with more porosity.[2] In this direction, a large number of MOFs with four-connected topological networks have been synthesized. Normally, square-planar four-connecting nodes will result in 2D **sql** (4^4), 3D $CdSO_4$ (**cds**, 6^58), NbO (**nbo**, 6^48^2), and **lvt** (4^28^4) nets, while tetrahedral nodes promote the formation of 3D diamond (**dia**, 6^6), $SrAl_2$ (**sra**, 4^26^38), and quartz (**qtz**, 6^48^2) nets.[3] In comparison, the binodal networks with mixed tetrahedral and square-planar tectons have been less known, most of which show moganite [**mog**, $(4.6^4.8)_2(4^2.6^2.8^2)$] and PtS (**pts**, 4^28^4) types. Currently, the preparation of MOFs with binodal four-connected and zeolite-type topological nets represents a potential challenge.

The oxalate dianion ($C_2O_4^{2-}$, ox) normally behaves as a typical bis-bidentate ligand to bridge homo- and/or heterometal ions, which has been widely employed to prepare metal oxalato systems with different stereochemistry and chirality.[4,5] Oxalato-involved MOFs have received considerable attention, mainly in the realm of molecular magnetism owing to its reliable ability to mediate significant exchange interactions. However, porous MOFs with oxalate tectons, which may be applied as multifunctional hybrid materials, are quite rare.[6] Moreover, oxalato-based coordination systems can be extensively developed with the aid of organic coligands.[7] In this connection, we have systematically explored the coordination assemblies of a bent dipyridyl building block 2,5-bis(4-pyridyl)-1,3,4-oxadiazole (4-bpo), which is a good candidate for constructing polymeric networks.[8] Herein, we will present a ternary system of copper(II) oxalate with 4-bpo as the coligand, which shows a pillared-layer 3D microporous framework with zeolite-type NiP_2 topology.

Blue block crystals of $\{[Cu_2(4\text{-bpo})(ox)_2](H_2O)_4\}_n$ (**1**) were obtained by the hydrothermal reaction of $Cu(NO_3)_2\cdot 3H_2O$, oxamide, and 4-bpo.[9] The oxalate anions in **1** should originate from the in situ hydrolyzation of oxamide,[10] and similar synthetic cases for metal oxalato systems have been known.[11] However, when oxamide is replaced with oxalic acid, an unknown precipitate is obtained instead under similar conditions. The composition and phase purity of complex **1** were characterized by IR spectrum, microanalysis, and powder X-ray diffraction (PXRD).

Single-crystal X-ray diffraction analysis[12] reveals that complex **1** has a pillared-layer 3D network, the asymmetric unit of which consists of one Cu^{II} center, half of a 4-bpo ligand, two half-occupied oxalate anions, and two lattice water molecules. Each Cu^{II} ion is six-coordinated to one pyridyl nitrogen from the bidentate 4-bpo ligand as well as five oxygen donors provided by one μ_2-oxalato and two μ_4-oxalato ligands (see Figure 1a). As expected, the $CuNO_5$ octahedral coordination sphere exhibits an elongated distortion, where the Cu1−N1/O2/O4/O5A lengths in the equatorial plane are obviously shorter than those of Cu1−O3B/O3C in the axial sites (see CIF for details). The bidentate 4-bpo ligand crosses a crystallographic 2-fold rotation axis that passes through O1 and the center of N2−N2A along $(0, y, {}^1/_4)$. The dihedral angle between two terminal pyridyl rings is 18.6(2)°, making a dihedral angle of 9.7(2)° with the central oxadiazole plane. The Cu···Cu separation by μ_2-oxalato is 5.182(3) Å, and the corresponding value by μ_4-oxalato is 5.569(3) Å. Additionally, the μ_4-oxalato group also bridges another two Cu^{II} ions from the vertical direction with a Cu···Cu separation of 7.976(2) Å. A search of the Cambridge Structural Database (CSD)[13] shows that only four cases[14] have such a μ_4-oxalato anion (see Scheme S1 in the Supporting Information for coordination modes of oxalato) among all known copper(II) oxalate systems. Interestingly, both μ_2- and μ_4-oxalato groups are

Received: April 7, 2011
Published: June 23, 2011

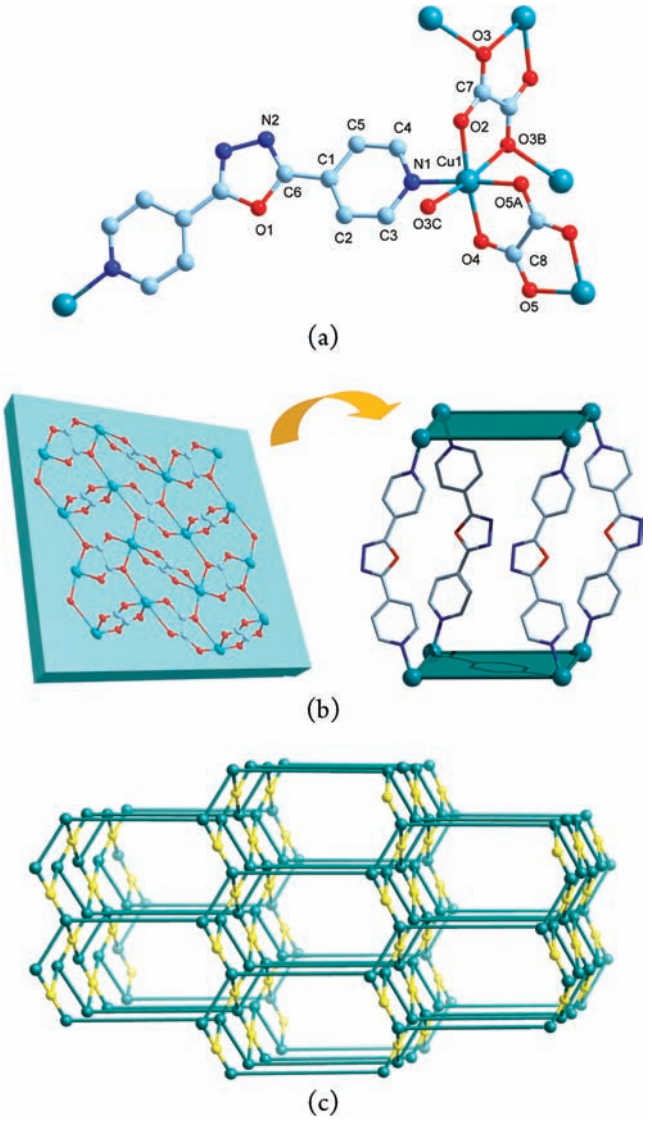

Figure 1. Views of **1**. (a) Local coordination geometry of Cu^{II} and the binding fashions of 4-bpo and oxalate (A, $-x + {}^1/_2, -y - {}^1/_2, -z$; B, $-x + {}^1/_2, -y + {}^1/_2, -z$; C, $-x + {}^1/_2, y - {}^1/_2, -z + {}^1/_2$). (b) 2D copper(II) oxalato layer (left) and 3D pillared-layer framework (right). (c) Schematic representation of the NiP_2 net topology (yellow spheres for μ_4-oxalate nodes and bottle-green spheres for Cu^{II} nodes).

centrosymmetric and link the Cu^{II} centers to construct a 2D $[Cu(\mu\text{-ox})]_n$ layer (see Figure 1b, left) along the *bc* plane, showing a (3,4)-connected **mcm** network with the point symbol of $(5^3)_2(5^4.8^2)$.[3]

In fact, a further extension of the neighboring $[Cu(\mu\text{-ox})]_n$ layers via the 4-bpo spacers results in a 3D pillared-layer framework (see Figure 1b right) with small 1D channels along the [001] axis (see Figure S1 in the Supporting Information), which are occupied by the lattice water moieties. The nearest interlayer Cu···Cu separation by 4-bpo is 13.830(2) Å. If the water guests are excluded, a calculation using the *PLATON* program[15] shows a solvent-accessible volume of 581.6 $Å^3$ (26.6% of the unit-cell volume). In this 3D coordination network, both tetrahedral (for Cu^{II}) and square-planar (for μ_4-oxalato) nodes are observed in a ratio of 2:1, with all μ_2-oxalato and 4-bpo acting as the two-connected spacers. Thus, a unique binary four-connected network (see Figure 1c) with $(5^3.6^2.7)_2(5^4.8^2)$ topology is afforded, being equal to that of the zeolite-type NiP_2 material.[16]

The thermal stability of **1** was studied by thermogravimetric analysis (TGA; see Figure S2 in the Supporting Information), which reveals the elimination of lattice water guests in the temperature range of ca. 30−130 °C (obsd, 11.6 wt %; calcd, 12.0 wt %). The residual host framework remains intact until a sharp pyrolysis occurs in the range of ca. 225−250 °C, followed by a gentle weight loss ending at ca. 560 °C. The residue holds 27.0 wt % of the total sample and can be properly ascribed to CuO (calcd, 26.7 wt %). To further investigate the porosity of **1**, a freshly ground sample (100 mg) was heated inside a vacuum oven at 200 °C for 6 h to release the guest water molecules. After desolvation, the evacuated solid displays a PXRD pattern similar to that of the as-synthesized material (see Figure S3 in the Supporting Information), confirming the steadiness of the host framework. Additionally, the dehydrated sample can regain the solvent molecules and revert to the original material by soaking it in water for 24 h, which is also supported by the PXRD pattern and the weight gain of the sample (11.8 mg, 11.8 wt %).

From the magnetic viewpoint, complex **1** shows a very peculiar arrangement where each distorted octahedral Cu^{II} ion is connected to three oxalato groups in different manners, forming four types of Cu^{II}−oxalato−Cu^{II} topologies: equatorial−equatorial (A), equatorial−axial (B), syn−anti (C), and oxo(oxalate) (D) (see Figure S4 in the Supporting Information).[17] In the former two of these motifs, the oxalate anions serve as bis-bidentate ligands to result in a 1D zigzag chain. Considering the chelating coordination mode and also the metallic d orbitals involved, they can be classified as coplanar (when the x^2-y^2 orbitals of both neighboring Cu^{II} centers are in the plane of the oxalato bridge; A) and perpendicular (when the z^2 orbital of one Cu^{II} is in the same plane as the x^2-y^2 orbital of the neighbor; B).[18] In fact, two such patterns alternate regularly in the 1D chain along the [010] axis, and these chains are further interlinked by another two groups of bridges in syn−anti and oxo(oxalate) modes (C and D) in the final 2D layer.

Owing to the structural complexity of **1**, a rigorous treatment of the experimental magnetic data can only be possible by theoretical calculations (see below). Nevertheless, a straightforward estimation may be obtained by simplifying the number of interactions. Basically, the magnetic behavior of **1** will be dominated by coplanar Cu^{II}−oxalato−Cu^{II} units, in which the oxalato bridge is centrosymmetric with two short bond lengths at each Cu^{II} ion. Also, it may be acceptable to think that the contribution of other couplings (perpendicular or cross-link) is substantially reduced and even nearly zero because the z^2 orbitals are always engaged in these (ferromagnetic or antiferromagnetic) interactions to make them very weak.[18] This strategy allows us to fit this system by using a dinuclear model (see below). As a matter of fact, no reasonable fit can be obtained with an alternating chain model.

Variable-temperature direct-current (DC) magnetic susceptibility data (see Figure S5 in the Supporting Information) show a behavior characteristic for strong antiferromagnetically coupled Cu^{II} centers, dropping with a decrease in the temperature. The magnetic data could be fitted by using the Bleaney−Bowers expression for isotropically coupled dinuclear $S = {}^1/_2$ ions, based on the spin Hamiltonian $H = -JS_1S_2$ with an impurity term. The best-fit parameters are $J = -246\ cm^{-1}$, $g = 2.02$, $\rho = 0.035$, and TIP = 120×10^{-6}. Although this fit is not completely satisfactory, the obtained *J* value agrees well with that expected for a dinuclear Cu^{II}−oxalato−Cu^{II} system. The difference between

dx.doi.org/10.1021/ic200711e |*Inorg. Chem.* 2011, 50, 6850–6852

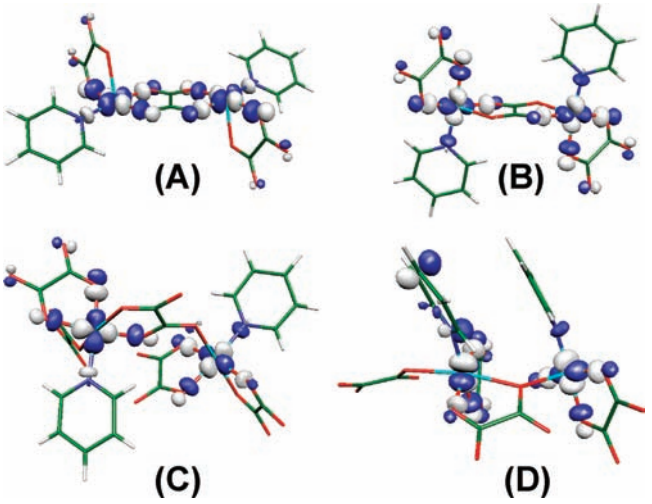

Figure 2. Views of the "in-phase" combination of the magnetic orbitals of different Cu^{II}−oxalato−Cu^{II} topologies obtained from the DFT calculations: (A) equatorial−equatorial, (B) equatorial−axial, (C) syn−anti, (D) and oxo(oxalate) bridges.

the experimental and fitting data suggests that the simplifications applied cannot be a priori disregarded at lower temperatures.

To fully understand the magnetic behaviors and obtain insights into the mechanism of exchange in **1**, density functional theory (DFT) calculations were performed to obtain the *J* values using the broken-symmetry procedure (see the Supporting Information for details). The calculated *J* value is $-204.9\ cm^{-1}$ for the equatorial−equatorial oxalato moiety, and that for the equatorial−axial oxalato moiety is $+4.4\ cm^{-1}$. In addition, the *J* values are $+12.4\ cm^{-1}$ for Cu^{II}−oxo(oxalate)−Cu^{II} and $-4.3\ cm^{-1}$ for Cu^{II}−O−C−O−Cu^{II} (syn−anti). As stated above, only the equatorial−equatorial bonds result in strong coupling between the magnetic orbitals, which can also be confirmed by spin density analysis (see Figure 2). On the other hand, when the magnetic coupling occurs between the equatorial and axial ligands, it will be weak, either ferromagnetic or antiferromagnetic, depending on the orthogonality of the corresponding magnetic orbitals.

In summary, we demonstrate herein a unique 3D pillared-layer MOF with a four-connected binodal NiP_2 network. The microporous host framework will be unchanged after the cycle of dehydration and rehydration. The novel Cu^{II}−oxalato−Cu^{II} topology and the associated magnetic exchange interactions have also been fully explored by both experimental and theoretical methods. This result may provide a potential route to the design and construction of multifunctional zeolite-type MOFs.

■ ASSOCIATED CONTENT

Supporting Information. X-ray crystallographic file (CIF), experimental and computational details, coordination modes of oxalato (Scheme S1), 3-D packing diagram (Figure S1), TGA curve (Figures S2), PXRD patterns (Figure S3), magnetic exchange interactions (Figures S4), and $\chi_M T$ vs *T* curve (Figure S5). This material is available free of charge via the Internet at http://pubs.acs.org.

■ AUTHOR INFORMATION

Corresponding Author

*E-mail: dumiao@public.tpt.tj.cn. Tel and Fax: 86-22-23766556.

■ ACKNOWLEDGMENT

This work was financially supported by the National Natural Science Foundation of China (Grants 20971098 and 21031002), Program for New Century Excellent Talents in University (Grant NCET-07-0613), Tianjin Natural Science Foundation (Grant 10JCZDJC21800), and Tianjin Normal University. J.R. and N. A.-A. acknowledge the Spanish Government (Grants CTQ2009/07264 and CTQ2009/06959), and N.A.-A. also thanks ICREA (Institució Catalana de Recerca i Estudis Avançats) for the financial support. J.R.-A. is thankful for the support of the Ramón y Cajal Program (Spanish Government).

■ REFERENCES

(1) Phan, A.; Doonan, C. J.; Uribe-Romo, F. J.; Knobler, C. B.; O'Keeffe, M.; Yaghi, O. M. *Acc. Chem. Res.* **2010**, *43*, 58.

(2) Flanigen, E. M. In *Introduction to Zeolite Science and Practice*; van Bekkum, H., Flanigen, E. M., Jansen, J. C., Eds.; Elsevier: New York, 1991; p 13.

(3) O'Keeffe, M.; Yaghi, O. M.; Ramsden, S. *Reticular Chemistry Structure Resource*; Arizona State University: Tempe, AZ, 2007; database available at http://rcsr.anu.edu.au/.

(4) Marinescu, G.; Andruh, M.; Lloret, F.; Julve, M. *Coord. Chem. Rev.* **2011**, *255*, 161.

(5) Gruselle, M.; Train, C.; Boubekeur, K.; Gredin, P.; Ovanesyan, N. *Coord. Chem. Rev.* **2006**, *250*, 2491.

(6) (a) Prasad, P. A.; Neeraj, S.; Natarajan, S.; Rao, C. N. R. *Chem. Commun.* **2000**, 1251. (b) Zhang, L.-Z.; Gu, W.; Li, B.; Liu, X.; Liao, D.-Z. *Inorg. Chem.* **2007**, *46*, 622. (c) Lu, W. G.; Jiang, L.; Lu, T. B. *Cryst. Growth Des.* **2010**, *10*, 4310.

(7) Clemente-León, M.; Coronado, E.; Martí-Gastaldoz, C.; Romero, F. M. *Chem. Soc. Rev.* **2011**, *40*, 473.

(8) Du, M.; Bu, X.-H. *Bull. Chem. Soc. Jpn.* **2009**, *82*, 539 and references cited therein.

(9) See Supporting Information for synthesis and characterization of **1** in detail.

(10) Oxamide can be converted to ammonium oxalate and oxalic acid by heating it for long periods with water; the best results are obtained by the application of pressure. See: Riemenschneider, W.; Tanifuji, M. Oxalic Acid. In *Ullmann's Encyclopedia of Industrial Chemistry*; Wiley-VCH: Weinheim, Germany, 2000.

(11) Ruiz, R.; Faus, J.; Lloret, F.; Julve, M.; Journaux, Y. *Coord. Chem. Rev.* **1999**, *193*−*195*, 1069 and references cited therein.

(12) Crystal data for **1**: $C_{16}H_{16}Cu_2N_4O_{13}$, $M_r = 599.43$, monoclinic, space group *C*2/*c* (No. 15), $a = 29.810(4)$ Å, $b = 9.1745(12)$ Å, $c = 8.3049(11)$ Å, $\beta = 105.891(2)°$, $V = 2184.6(5)$ Å^3, $Z = 4$, $D_c = 1.823\ g/cm^3$, $F(000) = 1208$, $R_{int} = 0.0240$, GOF = 1.046, $R_1 = 0.0363$, and $wR_2 = 0.0973$.

(13) Established by using CSD (version 5.31 of Nov 2009, plus five updates): Allen, F. H. *Acta Crystallogr., Sect. B* **2002**, *58*, 380.

(14) (a) Cavalca, L.; Villa, A. C.; Manfredo, A. G.; Mangia, A.; Tomlinson, A. A. G. *J. Chem. Soc., Dalton Trans.* **1972**, 391. (b) Mukherjee, P. S.; Konar, S.; Zangrando, E.; Diaz, C.; Ribas, J.; Chaudhuri, N. R. *J. Chem. Soc., Dalton Trans.* **2002**, 3471. (c) Keene, T. D.; Hursthouse, M. B.; Price, D. J. *Acta Crystallogr., Sect. E* **2006**, *62*, m1373. (d) Wen, G.-L.; Wang, Y.-Y.; Zhang, W.-H.; Ren, C.; Liu, R.-T.; Shi, Q.-Z. *CrystEngComm* **2010**, *12*, 1238.

(15) Spek, A. L. *J. Appl. Crystallogr.* **2003**, *36*, 7.

(16) In fact, a very similar copper(II) oxalato coordination framework has recently been reported in ref 14d, although the authors have not recognized the novelty of its network topology.

(17) This notation does not follow the IUPAC recommendations but will describe the exchange pathways more effectively.

(18) Cano, J.; Alemany, P.; Alvarez, S.; Verdaguer, M.; Ruiz, E. *Chem.—Eur. J.* **1998**, *4*, 476.